6. HELIOSEISMIC INVERSION FOR SOLAR STRUCTURE

Using the standard inversion procedure for the solar sound-speed profile of Kosovichev (1999), we inverted the 6,677 frequencies and their uncertainties that were computed by employing the MPTS method on the power spectra obtained from the $\mathcal{R}$2010_66 observing run to get the structural inversion shown in red in Figure 22. For comparison we overlayed in black the inversion profile shown in Figure 26 of Paper I that were obtained with the rev6 version of the WMLTP method when applied to an m-averaged spectral set derived from the $\mathcal{R}$2010_66 observing run. As can be seen, both inversions agree extremely well for fractional radii between 0.50 and the next-to-the-last point at the right. For both inversions the rightmost point is located at a fractional radius of 0.9976. The only difference near the surface between the two inversion profiles is the turn-around in the MPTS profile in comparison with the monotonically downward WMLTP profile. Most likely this difference is due to the use of different mode sets in the two inversions. In fact, while the MPTS profile is based upon frequencies up to 4600 μHz, the upper frequency limit used in the WMLTP inversion was 4500 μHz. The sharp decline for fractional radii below about 0.20 in the MPTS profile depends on lower degree modes. However, our 66-day observing run on which this profile is based upon is too short for getting sufficiently accurate lower degree mode frequencies to make either this decline or else the upward WMLTP profile as a real feature. We plan to investigate the sources of systematic errors that affect an inversion profile not only in the deeper interior but also close to the surface in an upcoming study. Such study requires, however, observing runs lasting longer than 66 days and which are, furthermore, from different epochs.

In spite of the differences between the MPTS and WMLTP profile, our conclusions drawn in Paper I remain still valid. First, there is a substantial deviation from Model S near the surface which coincides with the sub-surface rotational shear layer. Second, the stratification of the convection zone and heat transport properties may be significantly different from the predictions of the mixing length theory (see, for example, Vitense (1953)). Third, the sound speed in both the outer half of the convection zone and in the sub-surface shear layer is systematically lower than the sound speed in the standard solar model.

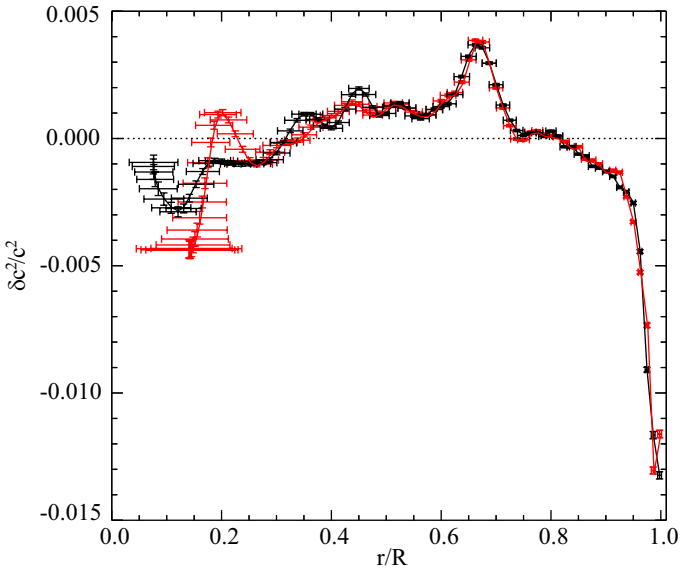

Figure 22. In red are shown the relative squared sound-speed deviations from the Standard Solar Model S of Christensen-Dalsgaard et al. (1996) in the sense "Sun minus Model" as a function of fractional radius that we obtained by a structural inversion of the 6,677 frequencies and their uncertainties that were computed using the MPTS method on the power spectra obtained from the $\mathcal{R}$2010_66 observing run. The frequency range extends from 965 to 4600 μHz (cf. upper-left panel of Figure 18). The horizontal bars represent the width ("spread") of the localized averaging kernels, providing a characteristic of the spatial resolution, while the vertical bars are the $1\,\sigma$ formal error estimates. For comparison are shown in black the relative squared sound-speed deviations from Model S that we obtained by a structural inversion of the 6,366 frequencies and uncertainties thereof that were computed using the rev6 version of the WMLTP method on an m-averaged spectral set obtained from the $\mathcal{R}$2010_66 observing run which covered the frequency range from 969 to 4500 μHz (cf. Figure 26 in Paper I).

7. HELIOSEISMIC INVERSION FOR SOLAR ROTATION

Solar internal rotation lifts the degeneracy of oscillation frequencies with the same (n, l), and introduces frequency splittings. The magnitude of the frequency splittings is determined by the rotation rate in the region where a given mode is trapped. Since each mode of solar oscillation is trapped in a different region, it is possible to infer the rotation rate in the solar interior as functions of radial distance and latitude by studying the frequency-splitting coefficients for all these modes.

The internal angular velocity distribution which resulted from this rotational inversion is shown in Figure 23. We note that the observations extended over more than two consecutive solar rotations, so that short-lived dynamical structures associated with individual active regions would have been averaged out of the inversion shown in Figure 23.

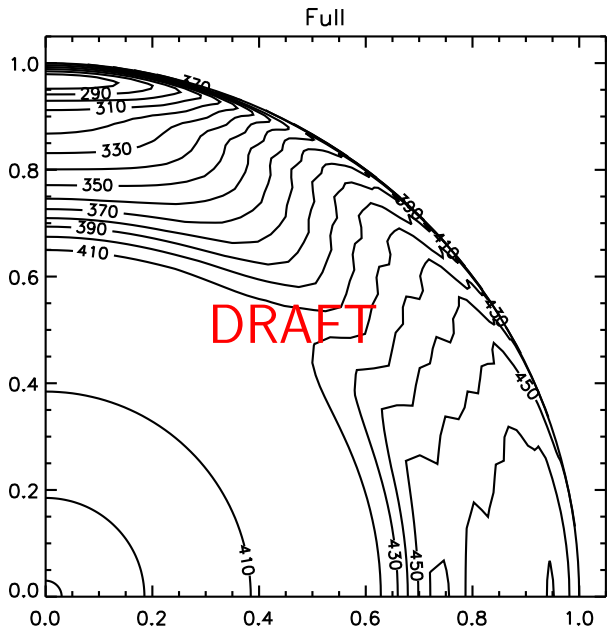

Figure 23. Internal angular velocity as functions of fractional radius and latitude from inversion of the set of MPTS frequency-splitting coefficients obtained from the $\mathcal{R}$2010_66 observing run.

TBD

8. CONCLUDING REMARKS AND OUTLOOK

Global helioseismology, that is the study of the Sun by means of its normal modes of oscillations, has revolutionized our knowledge of the Sun by revealing its large-scale structure and rate of rotation as functions of radial distance and latitude with unprecedented accuracy. However, what is still missing is an improved understanding of the near-surface layers of the Sun. These layers are believed to play a crucial role in the formation of the magnetic network, active regions, and sunspots, and thus are a key to the understanding of the mechanisms of solar activity and variability, at present possibly the most important unsolved problem in solar physics.

A straightforward approach to study the near-surface layers of the Sun is to employ precise frequencies of high-degree modes. Unfortunately, those modes do not appear as isolated, sharp peaks

in the power spectra but rather as broad ridges of power. This is mainly for two reasons. First, any power spectrum computed for a specific target mode (l, m) contains contributions of power from modes with neighboring l and m because the spherical harmonic functions used in the spatial decomposition of the observed Dopplergrams are not orthogonal on that part of the Sun we observe. These so-called spatial leaks are quantified by the leakage matrices. Second, with increasing degree the mode linewidth increases with both frequency and degree, while the frequency separation of the spatial leaks decreases. As a result, individual modal peaks blend together to form ridges of power. Since the amplitudes of the spatial leaks are asymmetric with regard to the target mode, the central frequency of a ridge is significantly offset from the target mode frequency. Therefore, the distribution of power in a ridge cannot be simply represented by using just a single symmetrical or asymmetrical function of frequency.

In Section 3 we have presented the mathematical details of how this issue can be overcome by employing a fitting profile that consists of a sum of individual overlapping profiles the relative amplitudes of which are governed by the leakage matrix appropriate to the targeted mode. The resulting fitting methodology we have given the name MPTS method. As is shown in Paper I, a similar approach has been implemented into the WMLTP method for the fitting of m-averaged spectra. Both the WMLTP and the MPTS method are equally well suited for the estimation of low-, medium-, and high-degree mode parameters, because they provide mode characteristics for both narrow modal peaks and broad ridges of power. However, while the frequency-splitting coefficients are an indispensable ingredient of the WMLTP method required for the generation of the m-averaged spectra, they are part of the results obtained from the MPTS method.

In Section 4 we have shown sample results obtained from the MPTS method. We have also displayed the sets of 6,677 frequencies, line widths, line asymmetries, and amplitudes that we generated by applying the MPTS method to the power spectra obtained from the $\mathcal{R}$2010_66 observing run. Moreover, in Section 4.1 we have been able to demonstrate that the multiplet structure of the f- and p-mode parameters as well as the shapes of the profiles fitted to the ridges of power are predominantly governed by the leakage matrices. This result reinforces the fact that the leakage matrices are crucial for the determination of accurate mode parameters.

In Section 5 we have thoroughly compared the results obtained from the MPTS method with those obtained from the WMLTP method (see Paper I), the WMLTP_ac method, the JS method (Schou 1992), and the SK method (Korzennik et al. 2004). Here, WMLTP_ac refers to a variant of the WMLTP method in which the segments of the raw spectra are collapsed into the m-averaged spectrum within the WMLTP code rather than collapsing them outside the code, using the frequency-splitting coefficients obtained from the MPTS method. In terms of frequency differences, line width differences, and a_1-splitting coefficient differences that were averaged in a weighted manner over all fitted ridges, we found that the MPTS method agreed best with the JS method with regard to all three average differences. The worst match was with the SK method in terms of the average frequency differences, with the WMLTP_ac method in terms of the average line width differences, and with the SK method in terms of the average a_1-splitting coefficient differences. In terms of the normalized frequency differences and the normalized a_1-splitting coefficient differences, we found the best agreement between the MPTS method and the JS method, while the worst match was between the MPTS and the WMLTP_ac method. In terms of the smoothness of the fitted mode parameters with respect to degree along a given ridge, as measured by means of the point-to-point

scatter defined in Equation (A1), we found that the MPTS method produced the smoothest results for both frequency and line width. Only in terms of the a_1-splitting coefficient was the JS method superior to the MPTS method.

Because the frequency and the frequency-splitting coefficient uncertainties are important input quantities in structural and rotational inversions, respectively, we have also compared those quantities produced by the various fitting methodologies. We have found that the averaged frequency uncertainties scaled as MPTS : WMLTP : WMLTP_ac : JS : SK = 1 : 0.8 : 0.7 : 2.3 : 8.6. For the averaged line width uncertainties the scaling factors were 1 : 1.4 : 2.0 : 1.2 : 0.6, and for the averaged a_1-splitting coefficient uncertainties we found the ratios MPTS : JS : SK = 1 : 1.6 : 4.3.

In Section 6 we have shown the results from a standard inversion procedure for the solar sound-speed profile, using the 6,677 frequencies along with their uncertainties that were computed by employing the MPTS method on the power spectra obtained from the $\mathcal{R}$2010_66 observing run. This inversion has been compared with the inversion profile shown in Figure 26 of Paper I that were obtained with the rev6 version of the WMLTP method when applied to an m-averaged spectral set derived from the very same observing run. Significant differences between the two inversions were to be noted near the surface as well as near the core, while in between the agreement was within the error bounds. The differences in the sub-surface layers are most likely caused by the fact that the sets of frequencies used for the two inversions had different upper frequency limits, viz. 4600 μHz for the MPTS profile, and 4500 μHz for the WMLTP profile. The differences near the core are an issue with the lower degree modes. Unfortunately, our 66-day observing run, $\mathcal{R}$2010_66, on which both profiles are based upon is too short for getting accurate enough lower degree mode frequencies to make either the downward MPTS profile or else the upward WMLTP profile as a real feature. In spite of the differences between the MPTS and WMLTP profile, our main conclusions drawn in Paper I remain still valid, namely a structural inversion including high-degree modes resolves the structure of the upper convective boundary layer with an unprecedented accuracy, and shows there a substantial sharp deviation from the adiabatic sound-speed profile of Model S. This is evidence that the stratification of the convection zone and heat transport properties may be significantly different from the predictions of the traditional mixing length theory, where near-surface turbulence effects may contribute as well.

In Section 7 we have shown the results from an inversion for solar rotation that, for the first time, takes into account frequency-splitting coefficients from high-degree modes up to $l = 1000$.

TBD

With the MPTS method a powerful tool for determining low-, intermediate-, and high-degree mode parameters including the frequency-splitting coefficients is available. We hope that this new method will lead to a renaissance of global helioseismology because it allows the addressing of the following important questions. First, investigation of temporal changes in the structure of the sub-surface layers in dependence of the solar cycle. Second, investigation of the effects of magnetic fields on the convective energy transport and irradiance variations in the course of the solar cycle by comparing the properties of the solar internal structure, as obtained from inversions for the adiabatic exponent, density, and the parameter of convective stability, with the results of realistic numerical 3D MHD simulations of the convective energy transport in the upper convection zone, carried out for different background magnetic field strengths, and by employing simultaneous irradiance measurements made by the SDO/EVE instrument. Third, determination of the solar heavy-element abundance. Recent

analyses of spectroscopic data have suggested that the heavy-element abundance Z needs to be revised downward significantly, from Z=0.017 (Grevesse & Sauval 1998) to Z=0.012 (Grevesse et al. 2007). This new value of Z results from the use of a 3D hydrodynamic model of the solar lower atmosphere instead of the classical 1D hydrostatic models, accounting for departures from local thermodynamic equilibrium (LTE) in the line formation, and improved atomic and molecular data. However, solar models constructed with this low heavy-element abundance do not satisfy helioseismic constraints. Rather they are found to have an incorrect depth of the convection zone, an incorrect helium abundance Y, and the sound speed and density profiles of the models do not match that of the Sun. This discrepancy constitutes of what is known as the "solar abundance problem". This has led to attempts to determine the solar heavy-element abundance utilizing helioseismic techniques (Antia & Basu 2006). However, so far those attempts were severely hampered by the lack of reliable high-degree mode frequencies.

In this work we utilized data from the Solar Oscillations Investigation / Michelson Doppler Imager (SOI/MDI) on board the Solar and Heliospheric Observatory (SOHO), and we have made use of NASAs Astrophysics Data System. SOHO is a project of international cooperation between ESA and NASA. The SOI/MDI project is supported by NASA grant NAG5-10483 to Stanford University. The portion of the research that was conducted at the University of Southern California was supported in part by NASA Grants NNX08A24G, NAG5-13510, NAG5-11582, NAG5-11001, NAG5-8545, NAG5-8021, NAG5-6104, and NAGW-13, by Stanford University Sub-Awards 14405890-126967, 1503169-33789-A, and 29056-C, by Stanford University Sub-Contract Number 6914, and by USC's Office of Undergraduate Programs. Part of this work is the result of research performed at the Jet Propulsion Laboratory of the California Institute of Technology under a contract with the National Aeronautics and Space Administration. J.R. is grateful to B. Vexler and D. Meidner of the Technische Universität München for their generous support and hospitality, and to K. Schittkowski of the University of Bayreuth for providing the source code of his `NLPQL` optimization technique. T.L. and J.R. are grateful to J. Christensen-Dalsgaard for providing us high-degree f- and p-mode eigenfunctions.

APPENDIX

A. ESTIMATION OF THE SMOOTHNESS OF FITTED PARAMETERS

In Appendix B of Paper I we suggested to measure the smoothness of a modal parameter υ with respect to degree l along a ridge of radial order n by the point-to-point scatter $\Sigma(\upsilon)$, as defined in Equation (B1) of Paper I. However, this definition has the disadvantage that it is independent of the uncertainty of the variable υ. Rather, it would be desirable that the contribution of the difference $\upsilon_{i+1} - \upsilon_i$ to the scatter $\Sigma(\upsilon)$ is weighted by its uncertainty in the sense that a small uncertainty increases the contribution to the scatter, while a large uncertainty decreases it. Therefore, we have revised the definition of the scatter, as follows:

$$\Sigma^2(\upsilon) = \frac{1}{2\,(l_{\max} - l_{\min})} \sum_{i=l_{\min}}^{l_{\max}-1} \frac{(\upsilon_{i+1} - \upsilon_i)^2}{\sigma_{i+1}^2 + \sigma_i^2}. \tag{A1}$$

Here, υ_i and σ_i are, respectively, the modal parameter and its uncertainty at degree i, and $l_{\min}$ and $l_{\max}$ are, respectively, the minimum and maximum degree l of the portion of interest of the ridge.